

## Tracking the Shadows through GMRT

D. Narasimha<sup>1</sup>, N. Kanekar<sup>2</sup> & J. N. Chengalur<sup>2</sup>

<sup>1</sup>Tata Institute of Fundamental Research, Mumbai 400 005.

<sup>2</sup>NCRA, Tata Institute of Fundamental Research, Pune 411 007.

**Abstract.** The structures of faint high redshift galaxies cannot be observed directly. But if a luminous quasar is located farther along their line of sight, high resolution absorption lines offer a valuable and reliable probe to their structure. GMRT is suited to monitor the absorption spectra, if the redshifted neutral hydrogen or OH doublet fall in one of the windows of the telescope. We present the OH doublet absorption spectra for the system B0218+357, taken at GMRT this year at resolution of approx. 9.5 km/sec with an rms noise of the order of 1 mJy. Based on our study of the OH doublet and 21cm neutral hydrogen line we infer that, in the lensing spiral galaxy of B0218 + 357, neutral hydrogen and OH coexist in tenuous clouds and there is possibly a hole in the central part of the galaxy. In contrast, the gas is seen in high density clouds in the lens in an otherwise similar system PKS1830-211.

*Key words.* Gravitational lens, molecular absorption lines, quasar—  
B0218 + 357.

### 1. Introduction

Gravitational lensing has opened up a new probe to the structure of high redshift galaxies using their absorption lines. A typical spiral galaxy at redshift upwards of 0.5 will have sufficient projected surface mass density to cause multiple images of suitably located background source, though it might be too faint for detailed direct observations. However, when it is along the line of sight to a quasar forming multiple images of the background source, the copious amount of neutral or low ionization gas in the intervenous galaxy gives rise to absorption lines in the multiple images. A comparison of the relative strength, doppler width and profile as well as difference in the doppler velocity of the lines along the images will provide valuable information about the dynamics as well as structure of the galaxy. For instance, from the relative strengths of the multiple radio lines of OH, the star formation history or the distribution of gas can be inferred.

B0218+357 is a well-studied gravitational lens system having radio ring (Patnaik *et al.* 1993), for which many mm molecular absorption lines have been detected. It consists of two images of a flat spectrum radio source (AGN) separated by 340 milliarcseconds and the Einstein ring has a diameter of 335 milliarcseconds. The AGN at a redshift of 0.96 is lensed by a spiral galaxy of I magnitude 20 at a redshift of 0.685. The time delay between the images has been measured to be 11 days. This lens could be

very useful to determine the large scale geometry of the Universe because of the moderate redshift of the lens and a relatively low redshift of the source with respect to the lens. The inferred Hubble constant or other predictions for an Open Universe without cosmological constant and a Flat Universe with a cosmological constant will be considerably different for this lens system. It is possible to construct reasonable lens model for the system using a high sensitivity EVN+MERLIN image of the system at 1.7 GHz and accurate position of VLBA scale substructures (Narasimha, Patnaik & Porcas, in preparation).

High sensitivity and high resolution observations of the absorption lines in radio provide valuable probe of the lens in the following way: (1) From a chemical diagnostic of the various radicals like OH and doppler width of the individual lines formed within a cloud, the star formation history of the galaxy can be traced. (2) Measuring rotation curve of the lensing spiral galaxy at high redshift (Chengalur *et al* 1999). For a single component lens, the images as well as radio ring can constrain the lens model accurately; but in a spiral galaxy the bulge, disk and possible halo simultaneously act as lens for subarcsecond images; consequently, models explaining the observed features of the radio ring and images at a specified single redshift can differ from each other by an unknown mass of the dark halo which will change the time delay between the images without affecting any other observables. The absorption lines due to the images as well as ring in the system can be used to directly infer the gravitational potential of the lens galaxy and hence break this degeneracy. Accurate diagnostic of the rotation curve requires determination of the doppler position of the absorption lines due to the two compact images and a shallow absorption trough due to the ring which becomes strong at low frequencies.

## 2. Analysis of 21cm neutral hydrogen line

Redshifted neutral hydrogen 21 cm line was observed at Westerbork telescopes by A G de Bruyn in July 1998. The 3.48 km/sec/channel spectrum and its decomposition is displayed in Fig. 1. The broad but shallow component of the absorption profile due to the radio ring at approx 10 mJy level is evident in spite of the rms noise of 1 mJy. It is tempting to identify the two narrow features in the profile as due to the compact images. However, the position of the absorption line is not at the centre of the radio ring and hence, neither of the features is likely to be due to the Image B. Instead, we interpret the two main features as lines arising from the two VLBA components of Image A. The derived line of sight rotation velocity at 0.18 arcsecond from the lens centre is approximately 70 km s<sup>-1</sup>. Since the lens is at an inclination of the order of 25 to 35 degrees, the total rotation velocity should be 150 km s<sup>-1</sup> at this radius.

## 3. GMRT observations

The first OH observation of B0218+357 was carried out at GMRT during 1999, but due to the high noise level of about 10 mJy, only the broad lines could be identified. Consequently, the observations were repeated on the 17th and 27th of June, 2001, with the standard 30 station FX correlator as the backend. A total bandwidth of 4 MHz was used for the observations, to include both the main OH transitions (at rest

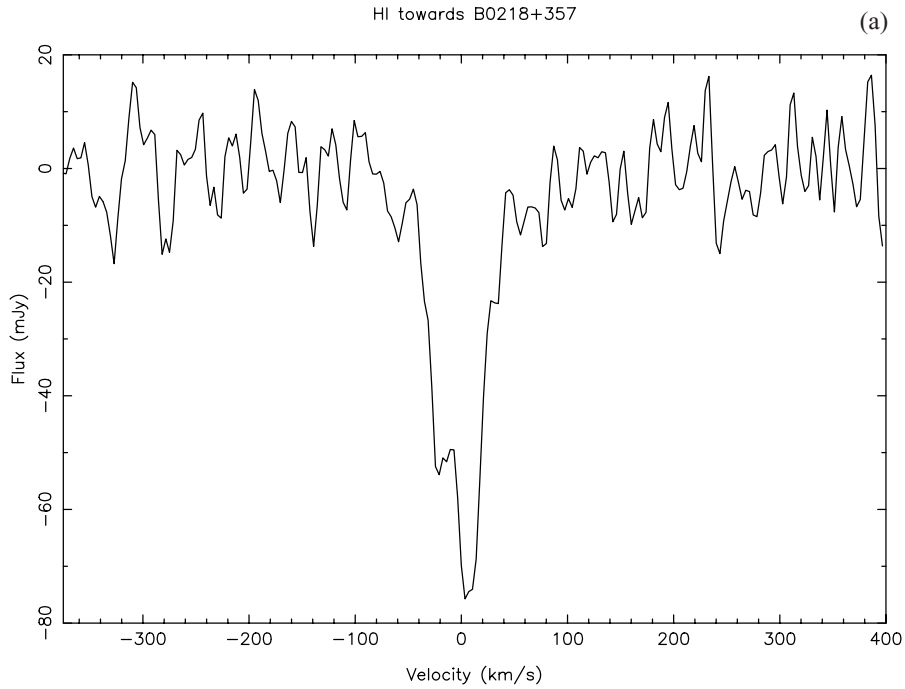


**Figure 1.** (a) Westerbork HI spectrum towards 0218+357. The spectrum has a resolution of  $\sim 3.48 \text{ km s}^{-1}$ .

frequencies of 1665.403 MHz and 1667.359 MHz). This was further sub-divided into 128 channels, yielding a velocity resolution of  $\sim 9.4 \text{ km s}^{-1}$  on each run. Twenty three and seventeen antennas were available for the observations on the 17th and the 27th respectively, due to various debugging and maintenance activities. The standard calibrator 3C48 was used to carry out absolute flux and bandpass calibration. Total on-source times were three and five hours on the first and second observing runs respectively.

The data were converted from the telescope format to FITS and analysed in AIPS. Data from the two days were analysed separately. Continuum emission was subtracted by fitting a linear polynomial to the U-V visibilities, using the AIPS task UVLIN. The continuum-subtracted data were then mapped in all channels and spectra extracted at the quasar location from the resulting three-dimensional data cube. The spectra of the two epochs were corrected to the heliocentric frame outside AIPS and then averaged together. The flux density of B0218+357 was measured to be 1.64 Jy at both epochs. Earlier experience with the GMRT indicates that the flux calibration is reliable to  $\sim 15\%$ , in this observing mode.

The final GMRT OH spectrum towards 0218+357 is shown in Fig. 2. The RMS noise is 1.1 mJy, per 9.4 km/sec/channel; note that the spectrum has not been smoothed. Both OH transitions are clearly visible; the peak absorption occurs at heliocentric frequencies of 988.56 MHz and 989.72 MHz, corresponding to redshifts  $z = 0.68467 \pm 0.00005$  and  $z = 0.68468 \pm 0.00005$  for the 1665 MHz and 1667 MHz transitions respectively.

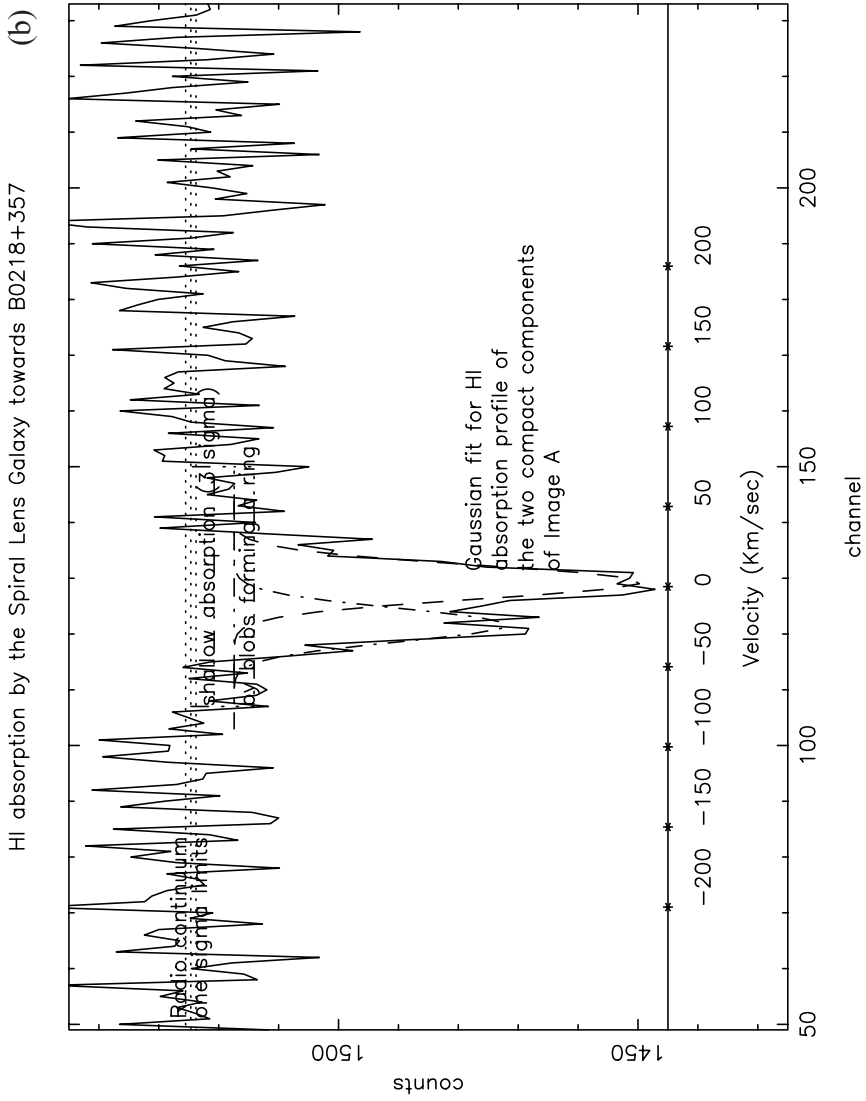


**Figure 1.** (b) Decomposition of the HI 21 cm line profile into main absorption feature in front of Image A as well as shallow absorption trough due to the radio ring. The best fit continuum and the shallow absorption level are shown along with the Gaussian main lines. The x-axis is the Doppler velocity with respect to the heliocentric frequency while the y-axis is the observed flux in mJy.

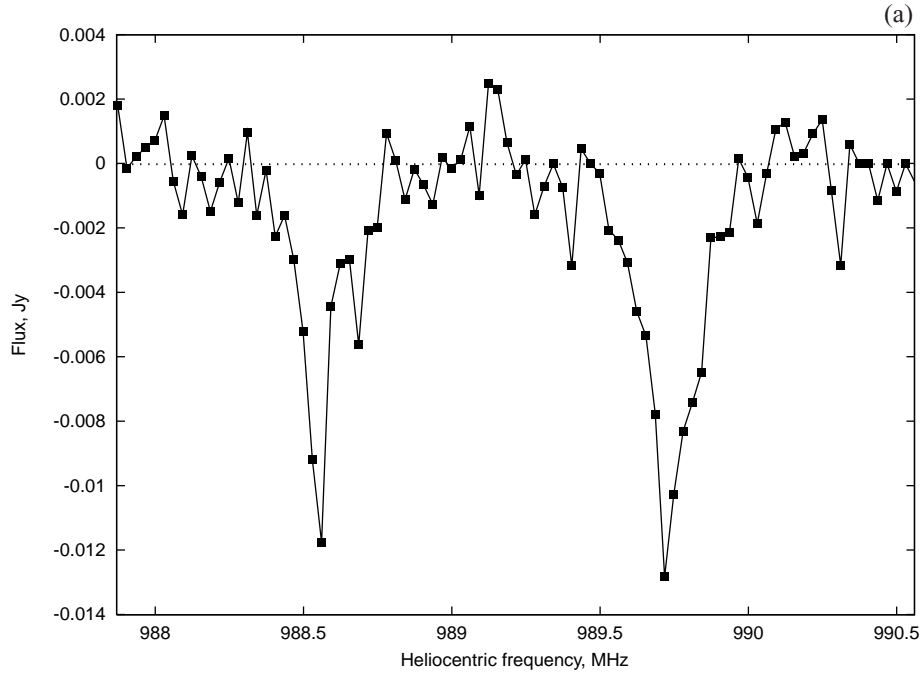


**Figure 2.** (a) GMRT 4 MHz OH spectrum towards 0218+357. The  $x$ -axis is heliocentric frequency, in MHz. The spectrum has a resolution of  $\sim 9.4 \text{ km s}^{-1}$ .

#### 4. Analysis of the OH line profiles and results

The spectral decomposition shown in Fig. 2 is similar to the HI line. In spite of the poor velocity resolution, absorption due to the radio ring can be extracted from both the OH lines at a doppler width of around  $70 \text{ km s}^{-1}$ . The inferred velocity at 1.4 kpc radial distance is between 120 and 160 km/sec, consistent with the HI value. But, like the HI line, absorption in front of Image B at the centre of the ring is absent in both the OH lines. So, the bulge of the lensing spiral galaxy appears to have a hole, a fact noted by Wiklind & Combes (1995).

The OH doublet have identical strengths as well as doppler width in front of Image A. Both the doppler position and velocity match well with the HI line. The inference is that neutral hydrogen and molecular gas appear to coexist, but in tenuous clouds where radiative equilibrium is established through infra-red pumping. This is in contrast with PKS1830-211, where a similar spiral galaxy at redshift of 0.89 has OH doublet of nearly 9:5 strength coexisting with neutral hydrogen, indicating that higher density gas clouds permeate the galaxy.

#### Acknowledgements

The OH observations were carried out with GMRT of TIFR.

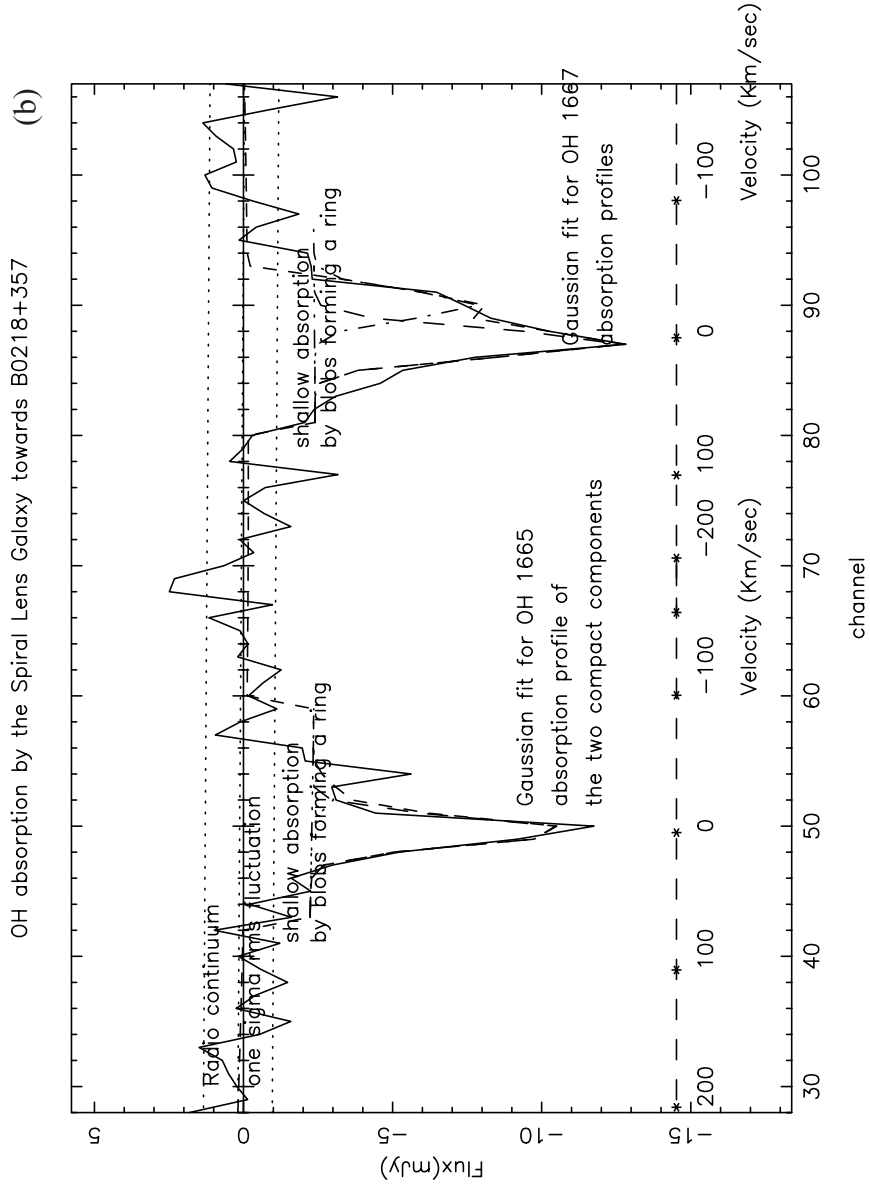


**Figure 2.** (b) Decomposition of the GMRT spectra into the main OH absorption feature in front of Image A as well as shallow absorption trough due to the radio ring. The best fit continuum and shallow absorption level are shown along with the Gaussian main lines. The x-axis is the Doppler velocity with respect to the heliocentric frequency while the y-axis is the flux in mJy.

**References**

- Chengalur, J., de Bruyn, A. G., Narasimha, D. 1999, *A&A*, **343**, L79.  
Patnaik, A. R. *et al* 1993, *MNRAS*, **261**, 435.  
Wiklind, T., Combes, F. 1995, *A&A*, **299**, 382.